Engineered Science
DOI: https://dx.doi.org/10.30919/es1181

Chemical and Morphological Characterization of PM_{10} in an Urbanized Valley in the American Tropics

Juliana Rojas Villa,[1,*] Mauricio A. Correa,[1] Luisa M.Gómez,[1] David Aguiar[1] and Henry A. Colorado[2,*]

Abstract

The present study focuses on the chemical and morphological characterization of PM_{10} (particulate matter ≤10 µm) in the Aburrá Valley surrounding the city of Medellin, Colombia, a significant location due to its geography and urbanization. Using scanning electron microscopy (SEM) with energy dispersive spectroscopy (EDS), PM_{10} samples were analyzed. This revealed a variety of particles that include iron and other metal oxides, calcium sulfates, fly ash, magnesium-rich particles, soot, aluminosilicates, carbonates, phosphates, mixed aluminosilicate-sulfate-carbonate particles, mixed aluminosilicate-carbonate particles, and biological matter. This research shows the specific physic-chemical characterization of PM for a large, and urbanized valley, which in some periods of the years has a complex air flow that traps gases that increases pollution in the city, enabling the formulation and planning of more effective policies for Colombia, but that can be extended to many countries with similar environmental issues.

Keywords: PM_{10}, Morphology; Metal oxides, Soot; Aluminosilicates; Scanning electron microscopy; Emission sources.
Received: 13 January 2024; Revised: 02 March 2024; Accepted: 06 March 2024.
Article type: Research article.

1. Introduction

Global concern about air quality and its adverse effects on health has prompted the development of different strategies to identify possible emission sources.[1] The deterioration of air quality is linked to the high percentage of the population residing in the world's major cities, which encourages the expansion of urban areas, the growth of industrial activities and the increase in vehicular traffic.[2] Exposure to high levels of air pollutants has adverse health effects, including respiratory and cardiovascular diseases.[3] Among the air pollutants recognized for their adverse health effects, particulate matter (PM) probably exerts the greatest influence on daily premature mortality rates. In addition, these pollutants are responsible for significant economy deterioration, accounting for 90% of the economic losses related to public health and air quality.[4]

PM is considered a complex mixture of particles of natural or anthropogenic origin that remain suspended in the atmosphere due to their small aerodynamic diameter (Dp).[5,6] Natural particles arise from soil erosion, emissions of biological material and forest fires. On the other hand, particles of anthropogenic origin come from human activity, such as combustion processes, industrial processes and vehicular traffic.[6] PM is classified according to its Dp into $PM_{2.5}$ (Dp < 2.5µm), PM_{10} (Dp < 10µm) and TSP (total suspended particulate matter).[3,6-8] $PM_{2.5}$ is composed of a large number of substances, such as inorganic compounds (metals, sulfates, nitrates, among others), organic compounds (soot, aromatic and polycyclic hydrocarbons), as well as biological elements such as pollen fragments and allergens.[9] Due to their size, PM penetrates deeply into the respiratory tract, causing lung cancer, cardiovascular, respiratory, and cerebrovascular diseases.[4] The relationship between air pollutants and mortality associated with the specific compounds of PM is established as follows from high to low: $PM_{2.5} > PM_{10} > SO_2 > H^+ > O_3 > NO_X$.[10]

According to the World Health Organization (WHO), the annual average of $PM_{2.5}$ in 2016 reached its highest value in Peru, followed by Paraguay, Colombia, Brazil, Argentina,

[1] *Grupo de Investigación y Laboratorio de Monitoreo Ambiental G-LIMA, Universidad de Antioquia UdeA, Calle 70 N-.52-21, Medellín 050010, Colombia.*
[2] *CCComposites Laboratory, Universidad de Antioquia UdeA, Calle 70 N-.52-21, Medellín 050010, Colombia.*
**Email:* mandres.correa@udea.edu.co (J. R. Villa), henry.colorado@udea.edu.co (H. A. Colorado)

Chile, and Ecuador.[11,12] In Colombia, 59 of the 78 municipalities with an air quality monitoring system reached concentrations of PM_{10} that were harmful to human health. For 2018, most regions under air quality monitoring exceeded the maximum allowable $PM_{2.5}$ threshold by 1.5 times the limit recommended by the World Health Organization (WHO). The Aburrá Valley Metropolitan Area (AMVA) stood out as one of the urban centers with the highest concentrations.[13] This problem is related to the geography of the Aburrá Valley (AV), which is located in a narrow and irregular mountainous area, characterized by steep slopes surrounding a valley. In addition, low wind speeds contribute to the formation of a stable microclimate that hinders the dispersion of pollutants. Every year, the AMVA presents problems associated with poor air quality, particularly during the February-March and October-November periods, which correspond to the first and second critical air pollution episodes, respectively. These episodes are related to the transition periods between the dry season and the rainy season.[13,14] By 2022, 83.77% of PM_{10} emissions from stationary sources registered by the environmental authority were generated by the beverage and food industry, the ceramics and vitreous industry, and the textile industry, the later being the sector with the highest contribution, accounting for 48.61% of these emissions.[15]

Formulating effective air pollution control policies faces a considerable challenge without a solid understanding of the major contributors to air pollutant concentrations.[9] The large number of possible emission sources, such as combustion, vehicular traffic, industrial activities, mining, metallurgy, biomass burning, and natural sources, makes the development of these policies feasible only if detailed information on the dimensions, morphology, and chemical composition of PM is available. In addition, the meteorological variables and the characteristics of the study area are also fundamental parameters.[16,17] In contrast, to bulk chemical analysis, scanning electron microscopy (SEM) with energy dispersive spectrometry (EDS) provide information related to the elemental composition, size distribution, reactivity, formation reactions, and the morphology of PM. SEM-EDS is an analytical method with a detection limit of 0.1 to 0.5% by weight for most elements, enabling the identification of emission sources.

During the last decades, SEM-EDS has been successfully used in the chemical and physical characterization of PM. Several chemical and morphological characterization studies, using SEM-EDS, have classified airborne particles (PM) into different groups according to their composition. These groups include aluminosilicates, silicates, iron mixtures, calcium sulfates, metal oxides, carbonates, silicate carbonates, soot particles, biological particles, carbon-rich particles, fly ash, tar balls, mineral particles, Na-Cl-rich particles, and fluorine-carbon-rich particles. This information is used to determine the physicochemical properties of PM and its different emission sources. For example, particles enriched with silica or silicates have been associated with long-range transport processes, coal burning, resuspension of soil dust, as well as construction activities. Aluminosilicates show a variety of morphological structures that depend on their composition and source of emission. Those of natural origin exhibit irregular morphologies, while those of anthropogenic origin have spherical shapes and are associated with fly ash. On the other hand, metal oxides with high Zn and Cu contents, with Zn-rich having spherical and Cu-rich irregular morphologies, are attributed to sources such as traffic.[9,10,18-29] Based on SEM-EDS analyses carried out in the Apulia region of Italy, the particles present at the sampling site were classified into thirteen different groups. The groups of particles classified as aluminosilicates, including those with sulfur, were found to be of natural origin. In the study area, very few spherical aluminosilicates particles of anthropogenic origin were found. As a result of their smooth surface, these particles were associated with coal fly ash.[30] A morphological analysis carried out in the city of Caracas, Venezuela, during the rainy season, classified the PM into seven groups. Among these groups are particles rich in Ti, Ca, Cl, and Mg. Within the category of Ca-rich particles, a subgroup consisting of calcite ($CaCO_3$) and dolomite ($MgCO_3.CaCO_3$), which are typical soil constituents, were identified. The morphology of these mineral particles is irregular with rough surfaces. On the other hand, Mg-rich particles are associated with soil dust resuspension, as well as with vehicular emissions.[6]

There are few morphological and chemical characterization studies of suspended particulate matter (PM) conducted in the Aburrá Valley, Colombia. One of these studies[31] revealed that the PM was composed of elements such as C, Si, Al, K, Ca, Na, Fe, Mg and Cu. The presence of Si is attributed to filter residues used in the collection of particulate matter, while C was associated with emissions from vehicles, domestic sources, and industry. In addition, Fe and Cu were found to be linked to industrial and vehicular sources.[31] Another study indicated that PM in the Aburrá Valley has a chain morphology and irregularly shaped particles, while different elements were found in PM_{10}, including Na, Al, Fe, Si, Cr and Pt.[32] Although these works made important contributions to the state of the art, the current research is a detailed analysis of the physic-chemical characteristics of the PM, facilitating to take more precise desitions to mitigate the current PM pollution.

The objective of this study is to determine the physical and chemical characteristics of PM_{10} by SEM-EDS, as well as to identify possible emission sources. This responds to the need to better understand the composition and sources of these particles in the specific context of the Aburrá Valley, Colombia. The research seeks to contribute to scientific knowledge about air pollution in this region, which is fundamental for the development of more effective air quality control policies, but also to make an impact on sites with similar geography and environmental problems worldwide.

2. Materials and methods

2.1. Study area

The sampling site is located in the AMVA, a subregion of the department of Antioquia, Colombia, with an area of 1152 km^2. It is made up of ten municipalities: Barbosa, Girardota, Copacabana, Bello, Medellín, Itagüí, Envigado, Sabaneta, La Estrella, and Caldas (Fig. 1). The MVA is located in the north of the central mountain range on an irregular topographic depression, with a narrow base (30 km wide on average) and steep slopes.[33] The climatic conditions of the VA are special, due to its irregular topography and the orographic barriers that limit the circulation of winds, and in turn hinder the dispersion of atmospheric pollutants.[33]

According to the National Administrative Department of Statistics (DANE) of Colombia, in 2018, the total number of inhabitants reached 3´726,219, evidencing an accelerated population growth linked to the rapid economic development in the area. This phenomenon is attributed to the presence of various industries, such as textiles, food, metal mechanics, among others.[15,34]

2.2 PM_{10} Monitoring

A total of 79 samples of particulate matter PM_{10} were collected (one of the main contributors to air pollution and with extensive availability of manual measurement data) at 10 separated stations of the Environmental Authority's air quality monitoring network (see Fig. 1, Table 1).[35] PM_{10} concentration was measured with manual high-volume (Hi-Vol) samplers, operating for periods of 24 hours ± 1 hour at a flow rate ranging from 1.02 to 1.24 m^3/min, following the protocols defined in US EPA CFR Title 40, Chapter I, Subchapter C, Part 50, Appendix J, High Volume, Manual Reference Method. The filters used were Whatman®1851-865 QM-A quartz fiber filters of 20 cm x 25 cm with a pore size of 2.2 micrometers (µm). All stations are equipped with meteorological devices to measure air temperature, relative humidity, wind direction, solar radiation, and wind speed.

The information was collected over several periods, from December 2018 through April 2019. The sampling period covered dates corresponding to environmental contingency periods established by the competent environmental entity, dates in which compounds associated with the use of pyrotechnic products are present, and dates in normal conditions of development of activities in the study area.

2.3 Morphological and chemical composition analysis (SEM-EDX)

Morphological and chemical composition analysis, including elemental mapping, was carried out using a Scanning Electron Microscope (thermionic) reference JEOL-JSM 6490LV.L, equipped with an INCA PentaFETx3 X-ray microanalyzer (Oxford Instrument). 79 samples of approximately 2 cm^2 were

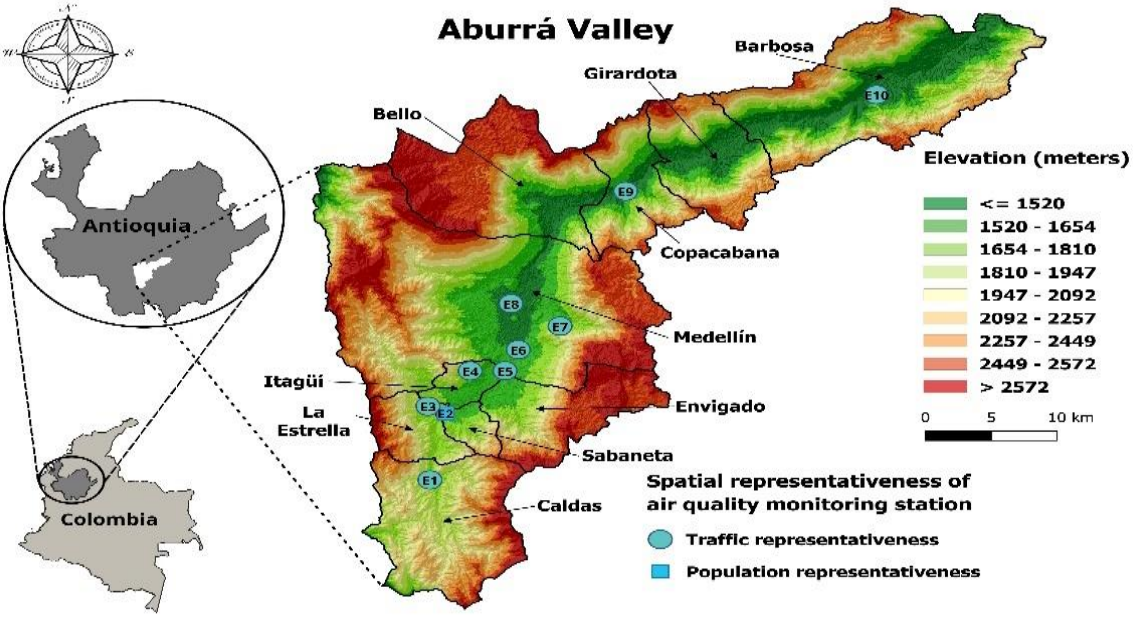

Fig. 1 Study area and location of air quality monitoring stations.

Table 1. SIATA PM_{10} air quality monitoring stations selected for the study arranged from north to south.

Township	Monitoring station		Type of station	Emission source
Barbosa	BAR-HSVP	Hospital San Vicente de Paúl	Suburban background	Wind regime
Copacabana	COP-HSMA	Hospital Santa Margarita	Suburban background	Wind regime
Medellín	MED-CORA	Corantioquia	Urban trend	Near busy roads and chain stores.
Medellín	MED-MIRA	Tanques Miraflores	Suburban background	Wind regime
Medellín	MED-PJIC	Politécnico Colombiano Jaime Isaza Cadavid	Urban traffic	Nearby traffic
Itagüí	ITA-PTAR	Planta de Tratamiento de Aguas Residuales	Urban industrial	Industrial emissions
Itagüí	ITA-POGO	Policía Los Gómez	Urban industrial	Emissions from ceramic industries
Estrella	EST-MAGO	Escuela Santa María Goretti	Urban industrial	Heavy industries, mainly in the metal-mechanic sector.
Estrella	SUR-TRAF	Tráfico sur	Urban traffic	Nearby traffic; major road corridors
Caldas	CAL-JOAR	Escuela Joaquín Aristizábal	Urban background	Wind regime

taken from the filter and fixed with graphite tape. Subsequently, they were coated with a thin layer of gold (Au) using the magnetron sputtering technique. The accelerating voltage was 20kV under high vacuum pressure during the equipment operation. The analysis methodology included image capture at lower magnification to obtain an overview of the filter and PM_{10} particles, followed by identification of areas of interest and spot magnification for detailed observation of different morphologies. Each morphology identified was subjected to energy dispersive spectroscopy (EDS) analysis to evaluate its chemical composition in specific areas and in the totality of the captured area, using elemental mappings. Subsequently, the most representative images were selected and classified into 11 different groups based on their chemical composition.

3. Analysis and results

Based on observations and analysis of numerous PM_{10} SEM-EDS images, 11 groups of particles with obvious morphological characteristics were identified. These particles are classified according to their elemental composition into metal oxides, iron oxides, calcium sulfates, fly ash, magnesium-rich particles, soot, aluminosilicates, carbonates, phosphates, mixed particles, and particles of biological origin.

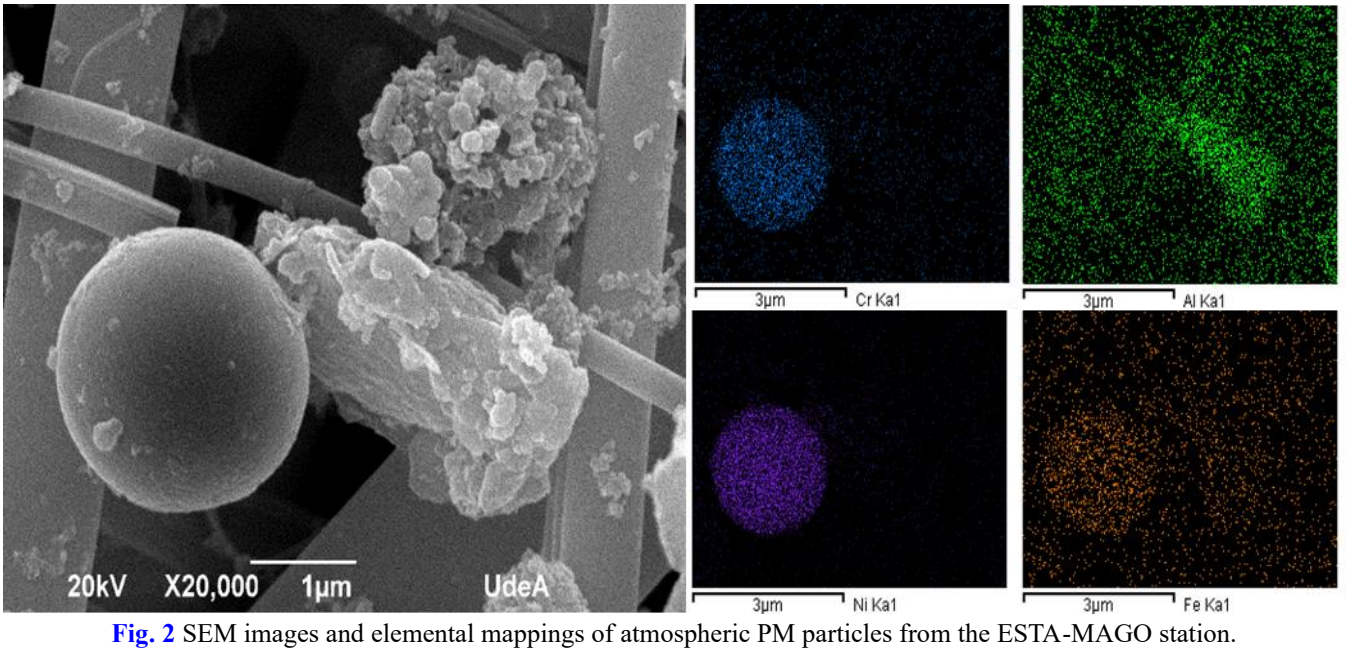

Fig. 2 SEM images and elemental mappings of atmospheric PM particles from the ESTA-MAGO station.

3.1 Metal oxides and Fe oxides

Figure 2 shows the PM_{10} SEM image of the EST-MAGO station. In this station, metallic oxides with a highly variable chemical composition, including Ni (33.81%), Cr (6.46%) and traces of Fe, Al, Na, Ti, K and Ca; with regular spherical morphology and diameter less than 2.5µm were identified. According to the literature, particles containing Al, Zr, Ni, and Mg are typically spherical, consistent with what has been found.[36] The presence of metals such as Cr, Ni, and Fe is linked to metalworking industries near the study site. The high Ni content is associated with the combustion of oils used in heavy industries with tall chimneys, close to the sampling site. On the other hand, Fe, Al, and Ca are generated by the resuspension of road dust.[37,38]

In addition, particles exhibiting smooth regular spherical morphologies suggesting a high Fe content were found, and these were classified as iron oxides, with sizes ranging between 1 to 8 µm. These particles were observed at stations EST-MAGO and MED-MIRA, Figs. 3a and b, respectively. Fig. 3a shows both spheres (Fe content 56.77%) and prismatic forms rich in Ca (19.81%), Al (10.17%), S, Na and K, indicating the presence of iron oxides and calcium sulfates, respectively. At the MED-MIRA station, iron oxides containing not only Fe (88.90%) and oxygen but also trace elements such as Na, Al, K, and Ca are found (Fig. 3b). Iron oxides usually present spherical morphologies with sizes that can vary between 1 and 50 µm, and sometimes they can even be encountered as smaller particles that join together to form spheres.[22,39] These Fe oxides result from high-temperature combustion processes generated by industrial plants near the EST-MAGO station. In addition, they can be suspended in the atmosphere from the ground surface as windblown mineral dust.[18,30]

3.2 Calcium sulfates

Figures 4a, b, c, d, and e show the SEM images and elemental mappings of the PM sampled at the ITA-PTAR, CAL-JOAR, and COP-HSMA stations. At these stations, symmetrical prismatic morphologies with sharp edges, typical of calcium sulfates such as $CaSO_4$ (gypsum), were observed. The chemical composition of the particles evaluated at these stations reveals high Ca (>60%) and S (>10%) contents, with some minor contributions of K, Al, Mg, Na, and Fe. According to the literature, the characteristic composition of calcium sulfates is defined by: Ca>70% and S>10%.[18,23,30] Consequently, the particle found corresponds to calcium sulfate.

In general, at the MED-MIRA, MED-PJIC, and SUR-TRAF stations, calcium sulfates were found with variable morphologies, such as bars, plates, needles, and some with irregular shapes (see Fig. 4). The formation of this compound in the stations mentioned above can be attributed to the deterioration of building surfaces and the desulfurization of flue gases which is due to the proximity of the stations to roads with high vehicular traffic, residential areas, and chemical industries.[40] In addition, they are generated from reactions between Ca-rich particles and S-containing compounds present in the atmosphere.[18,23]

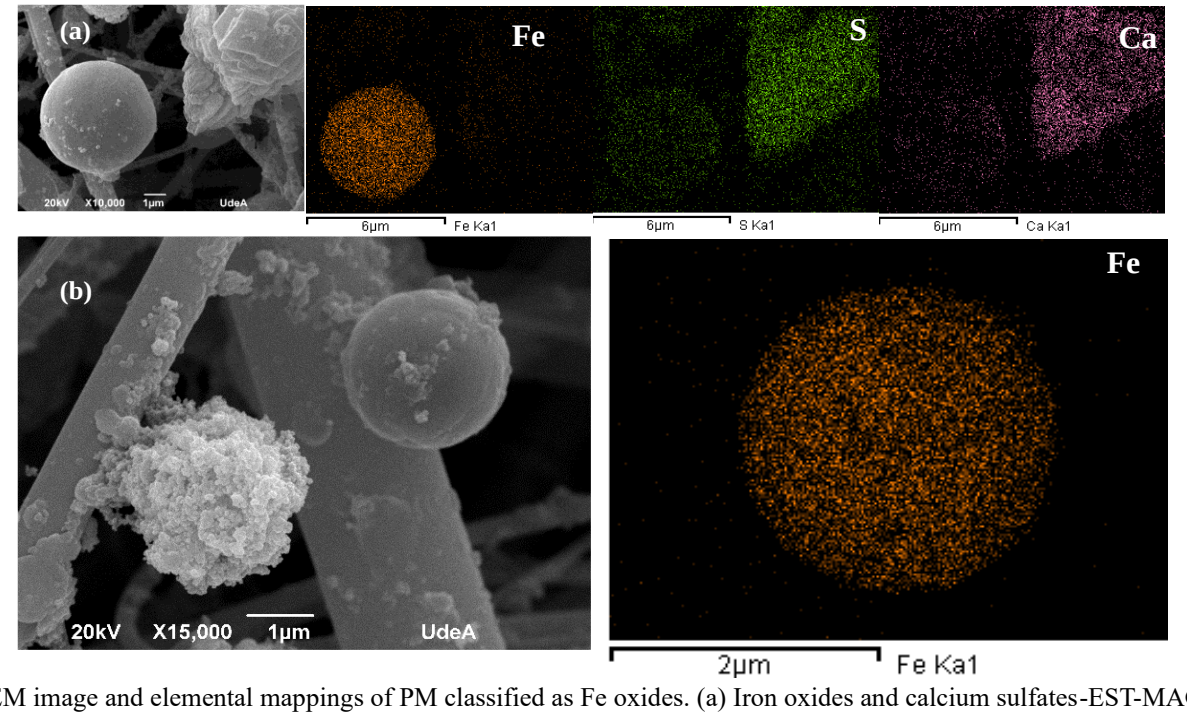

Fig. 3 SEM image and elemental mappings of PM classified as Fe oxides. (a) Iron oxides and calcium sulfates-EST-MAGO station, (b) Iron oxides-MED-MIRA station.

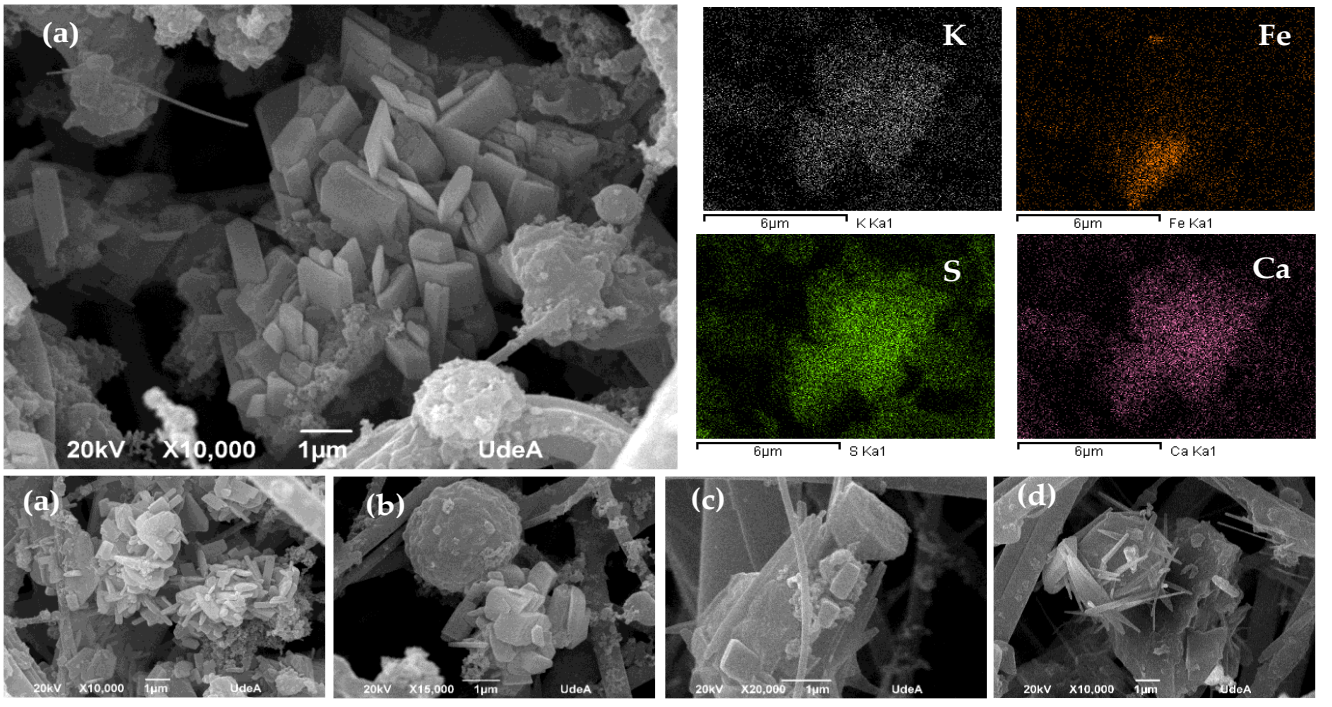

Fig. 4 SEM image and elemental mapping of PM classified as calcium sulfate. (a,b) ITA-PTAR, (c,d) CAL-JOAR, and (e) COP-HSMA.

3.3 Fly ash

The SEM with elemental mappings from SUR-TRAF, MED-MIRA, ITA-POGO, and SURF-TRAF stations are shown in Figs. 5a, b, c and d, revealing regular and spherical smooth-surfaced morphologies called fly ash. These are distinguished by their spherical shapes and smooth surfaces, which are generated by combustion processes associated with industrial activities near the stations evaluated. The composition of fly ash can vary, however, it usually contains aluminum oxide (Al_2O_3), silicon oxide (SiO_2), iron oxides (Fe_2O_3), calcium oxides (CaO), and magnesium oxides (MgO).[29] The elemental distribution in the spherical particles corroborates that they are fly ashes, because of their high content of Al, C, Ti, and trace elements such as Fe, Mg, Na, Ca, and K,[23,26] Fly ash is considered toxic due to the presence of metals, and in some cases chlorinated organic compounds.[9]

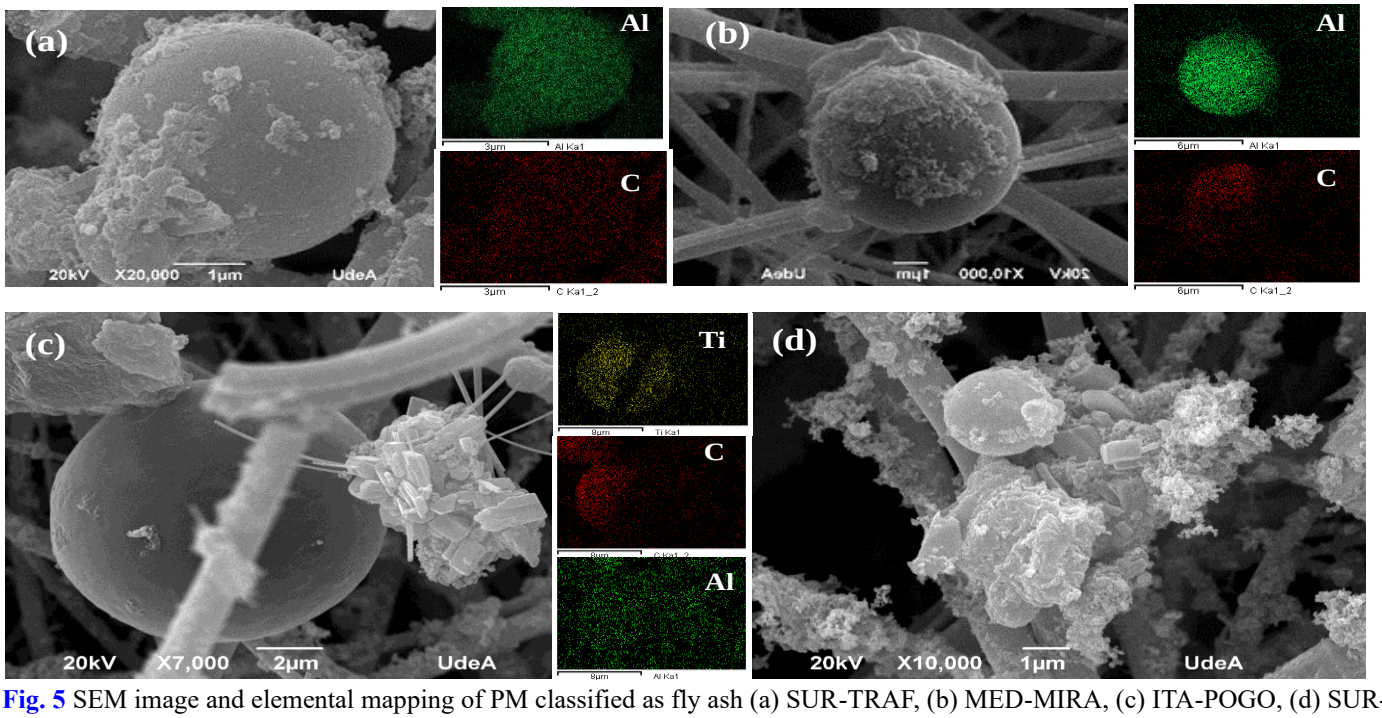

Fig. 5 SEM image and elemental mapping of PM classified as fly ash (a) SUR-TRAF, (b) MED-MIRA, (c) ITA-POGO, (d) SUR-TRAF.

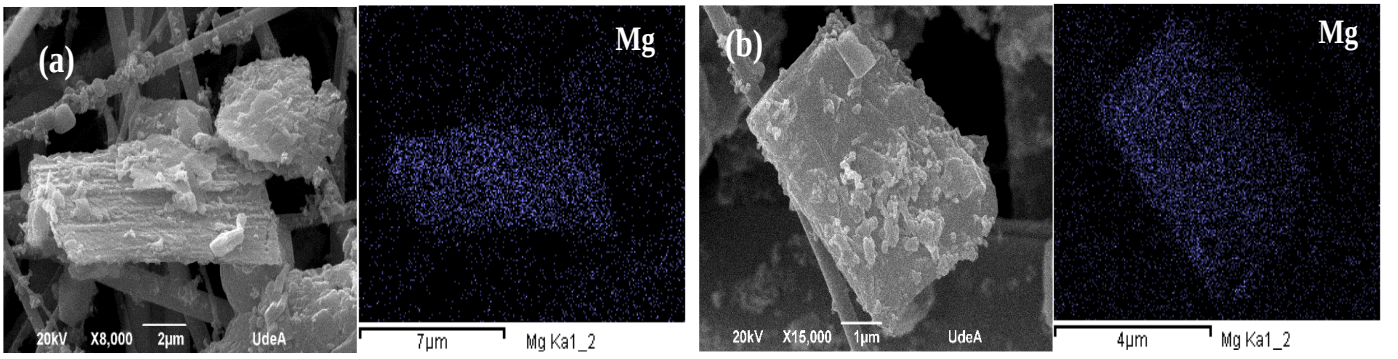

Fig. 6 SEM image of PM classified as Mg-rich particles (a) EST-MAGO, (b) SUR-TRAF.

Likewise, prismatic morphologies characteristic of calcium sulfates and soot aggregates are evidenced at stations ITA-POGO and SUR-TRAF, respectively (Figs. 5c and d). These stations are influenced by chemical, metal-mechanical, and agricultural industries, as well as by the high flow of vehicles.

3.4 Mg-rich particles

The Mg-rich particles found at stations EST-MAGO and SUR-TRAF showed trapezoidal sheet shapes with irregular surfaces and sizes greater than 7 µm (Figs. 6a and b). These particles have a variable chemical composition, with a high content of Mg (> 22%) and Al, in addition to other elements such as Na, K, Ca, Fe, and C. The irregular surface of these particles results from the presence of Al-rich agglomerates.

Particles with high Mg content are linked to soil dust that is suspended by wind and/or vehicle activity, this last one mainly caused by the SUR-TRAF station, which is strongly affected by traffic on highways with high vehicular flow.

3.5 Soot particles

Agglomerates of fine spherical carbonaceous particles with short chain structures and an average size of 0.34 µm were observed (see Figs. 7a, b and c). EDS analysis shows a high concentration of carbon (> 85%) and traces of Na, K, Ca, S, and Fe. These morphological and compositional characteristics are representative of soot. Soot morphology depends on combustion conditions, atmospheric processes, and fuel types. The emission of these particles comes from the burning of biomass or incomplete combustion of diesel. Due to their size, they have gained relevance today because of their contribution to climate change, decreased visibility, and adverse effects on human health.[9,10,23,30,41]

3.6 Aluminosilicates

Figs. 8a, b, c, d, and e show the morphological characteristics of the aluminosilicates found at the COP-HSMA, SUR-TRAF, CAL-JOAR, and BAR-HSVP stations. In general, irregular morphologies are observed, some of them with well-defined shapes. The composition of these particles is variable, with high fractions of Al and Si (Al + Si > 45%), including other elements from the earth's crust such as K, Mg, Ca, Na, and Fe. Fig. 8d shows irregular particles with Al (15.49%) and variations of Fe (9.82%), Mg (5.36%), K (5.67%), Ca (1.71%), and Ti (1.23%). This composition is generally associated with potassium feldspar-type aluminosilicates from natural sources, such as windblown dust, crustal material, and unpaved roads.[42,43] In addition, particles with prismatic morphology and a size of less than 2 µm are found, associated with sources such as abrasion, resuspension of minerals, and high temperature processes, such as those occurring in the ceramic and glass industry.[5,24] Fig. 8e shows a semispherical morphology with a smooth surface, enriched with Al (69.95%) and Na (12.49%), with traces of Fe, K, and Ca. This composition and morphology are typical of aluminosilicates of anthropogenic origin from ceramic industries.[24,44]

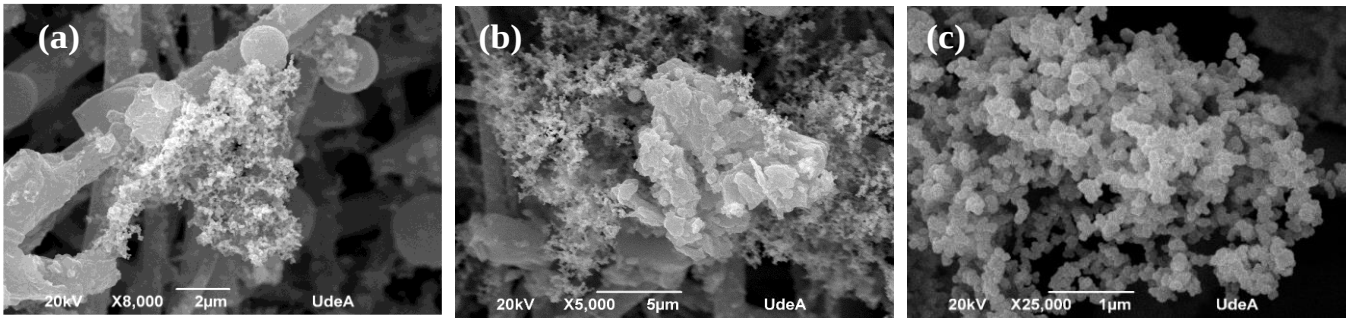

Fig. 7 SEM image of PM classified as soot. (a) MED-PJIC, (b) COP-HSMA, (c) ITA-POGO.

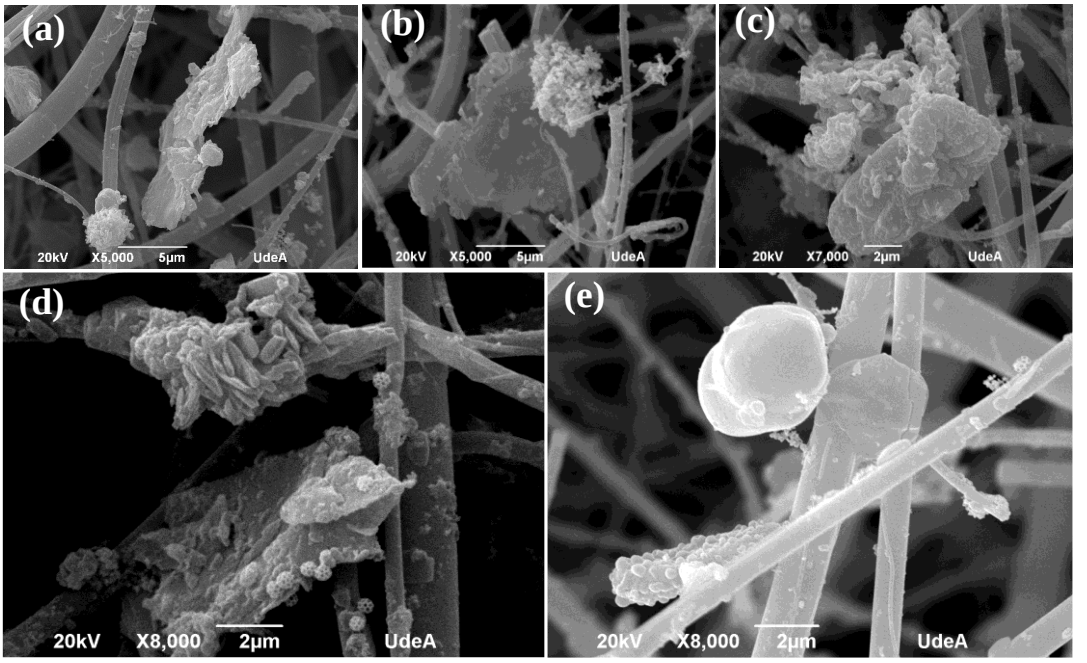

Fig. 8 SEM image of PM classified as aluminosilicates: (a) COP-HSMA (b) SUR-TRAF, (c) CAL-JOAR, (d and e) BAR-HSVP.

3.7 Carbonates

The calcium carbonates found in the particulate material from the ITA-POGO, MED-CORA and SUR-TRAF stations are characterized by their high Ca content (> 30%), as well as the presence of C and O, with traces of Na, Zn, Mg, and Al (Figs. 9a, b, c and d).

These carbonates have both irregular and regular morphologies, with some degree of symmetry, and sizes ranging from 5 to 10 μm. Particularly, at the ITA-POGO station, PM with irregular morphology rich in C (58.77%), Al (13.95%), and Fe (15.63%) were observed, with traces of K (3.87%), Ca (3.28%), Mg (2.07%), Na (1.30%), Ti (0.55%), Mn (0.59%), This indicates the presence of calcium carbonates, such as dolomite, possibly derived from the ceramic industry (see Fig. 9a). Fig. 9d, corresponds to the SUR-TRAF station, it shows irregular structures with sharp edges, rich in C (59.68%), Mg (15.35%), Al (13.57%), and Fe, Cr, Ca, K, Al, and Na. Metals such as Al, Cr, and Fe can cause toxic effects on living organisms.[36,45] Activities such as metal smelting, steel processing, ceramic and refractory industries are located in the vicinity of the SUR-TRAF station. Therefore, the chemical composition found can be linked to the presence of clay minerals, such as dolomite (CaMg and $(CO_3)_2$)metal oxides. On the other hand, carbonates from the MED-CORA station revealed Zn contents higher than 8%. The presence of Zn at this monitoring station is attributed to the wear and tear of some automobile parts (*e.g.*, brakes), and to vehicular emissions from nearby road corridors.[18]

3.8 Phosphates

The morphology of the phosphates from both the EST-MAGO and MED-PJIC stations is laminar with rounded edges (See Figs. 10a and b). Its chemical composition is characterized by high contents of Ca (48.67%), P (20.12%), Na (13.73%), with traces of Mg, Al, Fe, and K. These phosphorus particles are usually found in the form of $Mg_2P_2O_7$ and SiP_2O_7, and come from vehicle emissions. This is because several organic phosphorus compounds are used as corrosion inhibitors in fuels.[23]

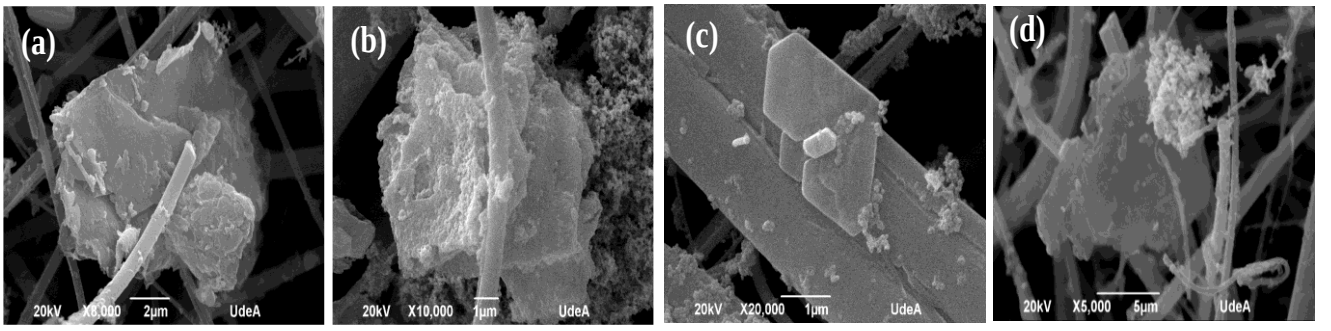

Fig. 9 SEM image of PM classified as carbonates (a) ITA-POGO, (b) MED-CORA, (c and d) SUR-TRAF.

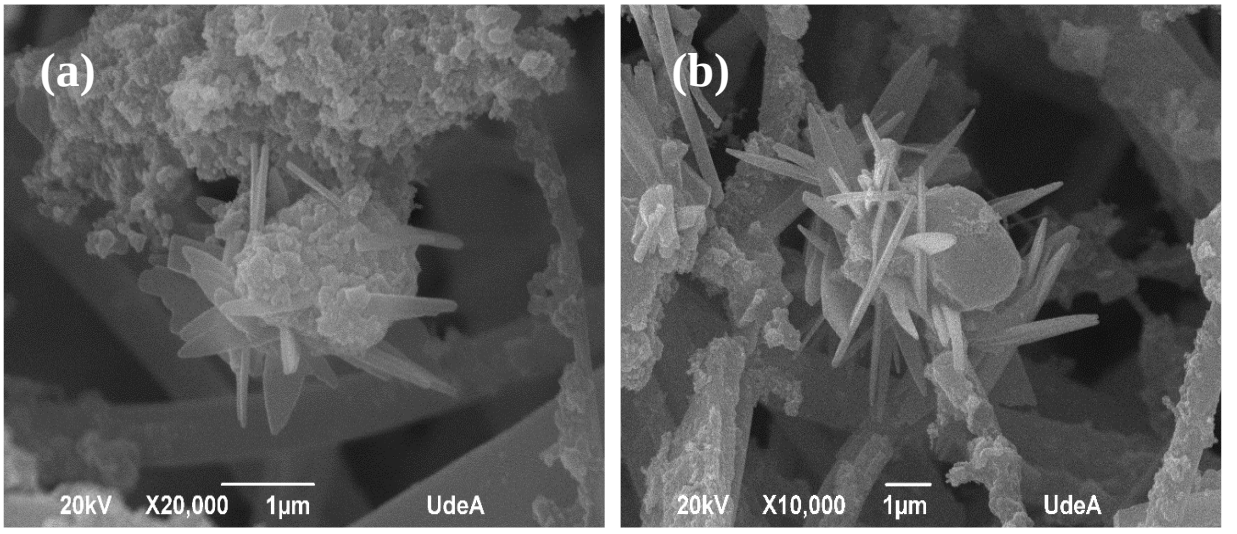

Fig. 10 SEM image of PM classified as calcium phosphates (a) EST-MAGO, (b) MED-PJIC.

3.9 Mixed particles

The mixed aluminosilicate-sulfate-carbonate particles are characterized by their formed aggregates, which have both irregular and regular morphologies, such as lamellae and rods (Figs. 11a, b, c and d). The main characteristic for categorizing these mixed particles is determined by their chemical compositions, which include elements such as S, C, Ca, Al, Si in higher proportions, while Na, Mg, K, Ti, Fe, and Mn are found in lower concentrations. Fig. 11a shows the presence of elements such as Al, C, Si, Ca, Fe, S, among others. Accordingly, these mixed particles are divided into three categories: sulfur-bearing aluminosilicates (Si+Al > 20% and S > 10%), calcium sulfates, and carbonates. The contribution of sulfate ion (SO_4^{2-}) in this type of particulate matter is related to the use of coal with high sulfur content in industries that use such coal as fuel.[46-48] The elemental composition of the particles found at the COP-HSMA station reveals the presence of Pb (2.74%).[24] According to the monitoring network of the

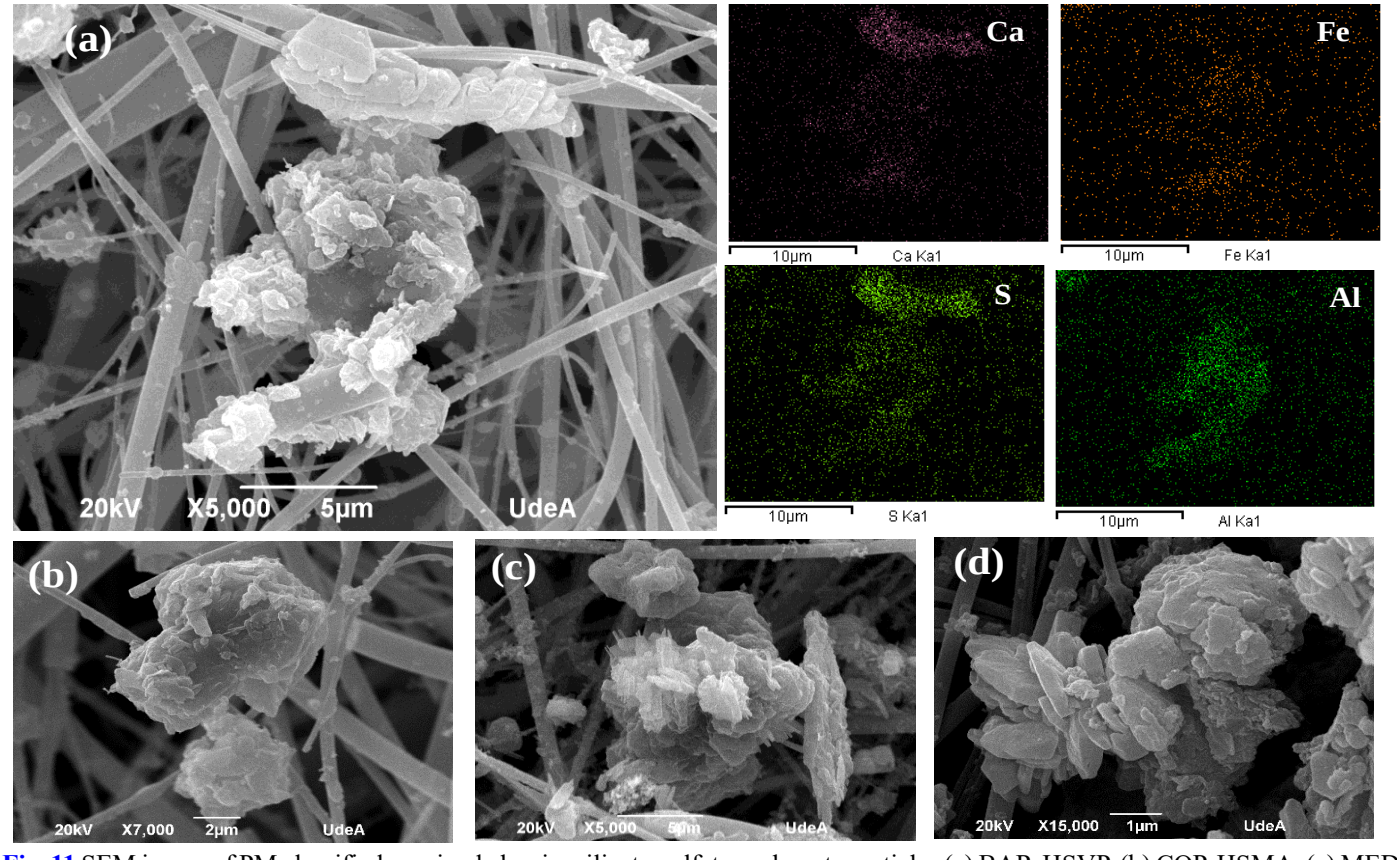

Fig. 11 SEM image of PM classified as mixed aluminosilicate-sulfate-carbonate particles (a) BAR-HSVP, (b) COP-HSMA, (c) MED-PJIC, (d) MED-MIRA.

environmental authority, this station is affected by the wind regime, mainly from the NNE and NE, which suggests the influence of anthropogenic sources such as refineries, vehicle emissions, power plants and ceramic industries.[49] These sources are associated with Pb-containing particles.

Mixed aluminosilicate-carbonate particles were found at stations ITA-POGO, ITA-PTAR and EST-MAGO, showing irregular and regular morphologies (Figs. 12a, b, c and d). Its composition is similar to the aluminosilicates and carbonates groups, with high fractions of Al, Si, C, and Ca predominating. Fig. 12a shows regular morphologies, such as prisms and elongated rods. Both this morphology and the detection of Al, Si, Na, Ca, Fe and K suggest the presence of mixed aluminosilicate and carbonate particles.[9] The morphology and chemical composition of the particles described indicate that the PM collected at the ITA-POGO and EST -MAGO stations is influenced by nearby industrial sources. These sources include ceramic industries that operate with various minerals such as dolomite, mullite, cordierite, among others.[50]

3.10 Biological particles

Biological particles of natural origin were also identified in the samples of Figs. 13a, b, c, and d. Diverse morphologies are evident, with sizes ranging from 0.3 to 10 µm. These particles are characterized by high carbon and oxygen fractions. Fig. 13a and Fig. 13d show spherical like honeycomb particles associated with brocosomes, a type of proteinaceous secretory particles with a size less than 1 µm. These are related to leafhoppers, which are coated with brocosomes to achieve a superhydrophobic exterior.[10,51,52]

3.11 Particle size distribution

Table 2 shows the average diameters of PM_{10} particles, obtained using ImageJ software. The standard deviation of particle diameter, recorded on date 2 (corresponding to pyrotechnic events) at various monitoring stations, reveals that the values of the data set are closer to the mean. This proximity suggests greater precision in particle diameter measurements made during this date. On the other hand, the higher standard deviations observed on dates 1 and 3 indicate a greater dispersion in the measurements made in those periods. For date 2, it was found that the average diameter of PM_{10} was 3.04 ± 1.43, smaller than the size on dates 1 and 3, with an average size of 4.12 ± 2.2 and 4.49 ± 2.67, respectively. The variation in particle sizes can be influenced by various emission sources, both natural and anthropogenic. For example, the smaller particles, such as fly ash, soot and calcium phosphates shown in Figs. 5, 7 and 10, are attributed to anthropogenic sources, such as vehicle emissions and industrial activities. In contrast, particles such as aluminosilicates and mixed particles, mainly of natural origin, exhibit larger particle sizes, as shown in Figs. 8, 11, and 12.

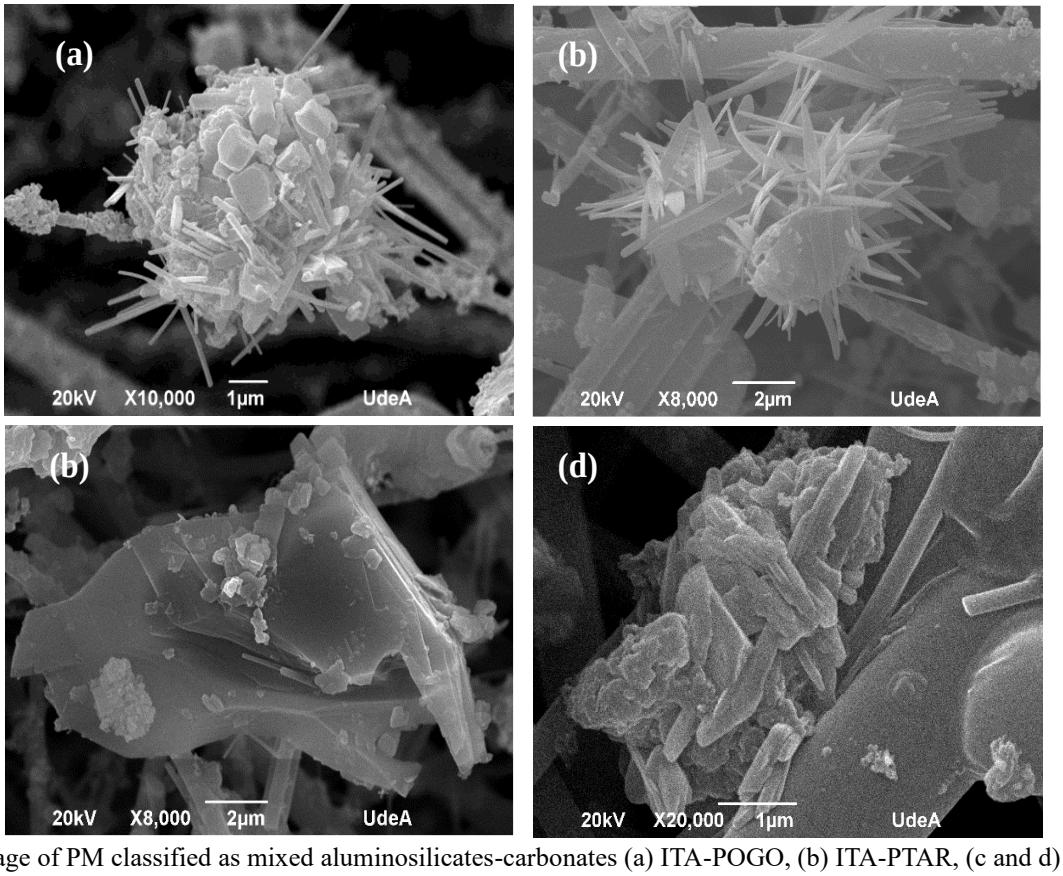

Fig. 12 SEM image of PM classified as mixed aluminosilicates-carbonates (a) ITA-POGO, (b) ITA-PTAR, (c and d) EST-MAGO.

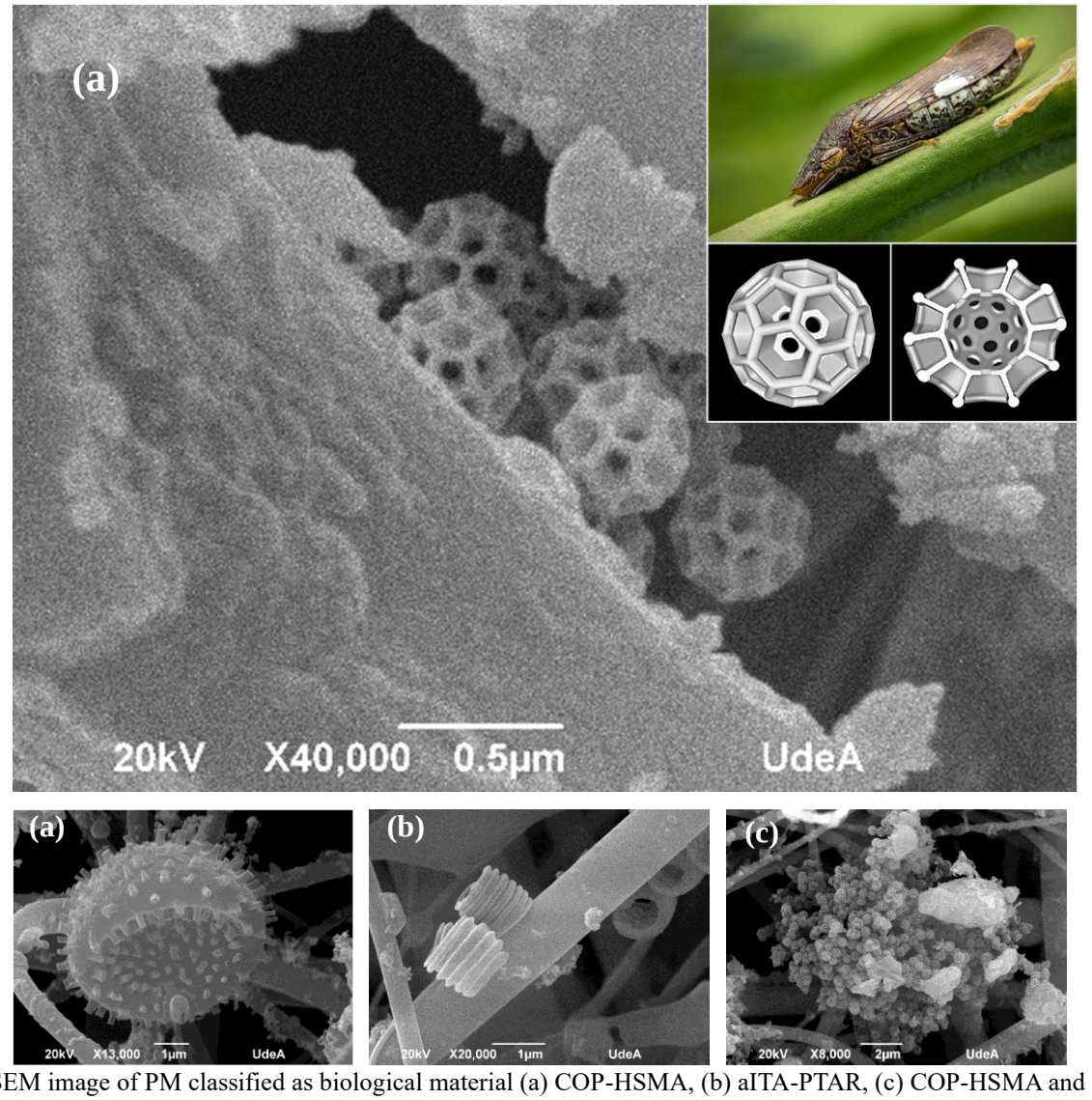

Fig. 13 SEM image of PM classified as biological material (a) COP-HSMA, (b) aITA-PTAR, (c) COP-HSMA and (d) EST-MAGO.

Table 2. Size distribution results measured on different sampling dates.

	Date 1	Date 2	Date 3
Mean	4.12	3.04	4.49
standard deviation (σ)	2.20	1.43	2.67
Maximum	14.52	9.48	13.67
Minimum	1.00	0.39	1.10

Histograms of PM_{10} particle size distribution are shown in Fig. 14. The histogram in Figs. 14a and b shows that most of the particles have a size between 2 and 6 µm, which is consistent with the definition of PM_{10}. On the other hand, the distribution shown in Fig. 14c indicates that the particles have an average size in the range of 1-5 µm, in accordance with the definition of PM_{10} (Dp < 10 µm). In general, the histograms in Figs. 14a, b, and c show that the highest number of particles is in the 2-4 µm range, sizes associated with anthropogenic sources. This result suggests that the particulate matter sampled is predominantly influenced by anthropogenic sources rather than natural sources.

4. Discussion

The identification of soot particles, with their chain structures and carbon-rich composition, points to the importance of controlling the incomplete combustion of fossil fuels. The presence of soot is of particular concern due to its ability to penetrate deep into the human respiratory tract, causing health problems such as cardiovascular and respiratory diseases.[3,7,8] This finding suggests the need to improve the combustion technologies in the examined valley, as exhaust emissions from internal combustion engines are a major source of environmental pollution. The development of technologies such as catalytic filters may be a promising option to reduce the levels of pollution emitted by these engines.[53,54] The characterization of fly ash and calcium sulfates, with spherical

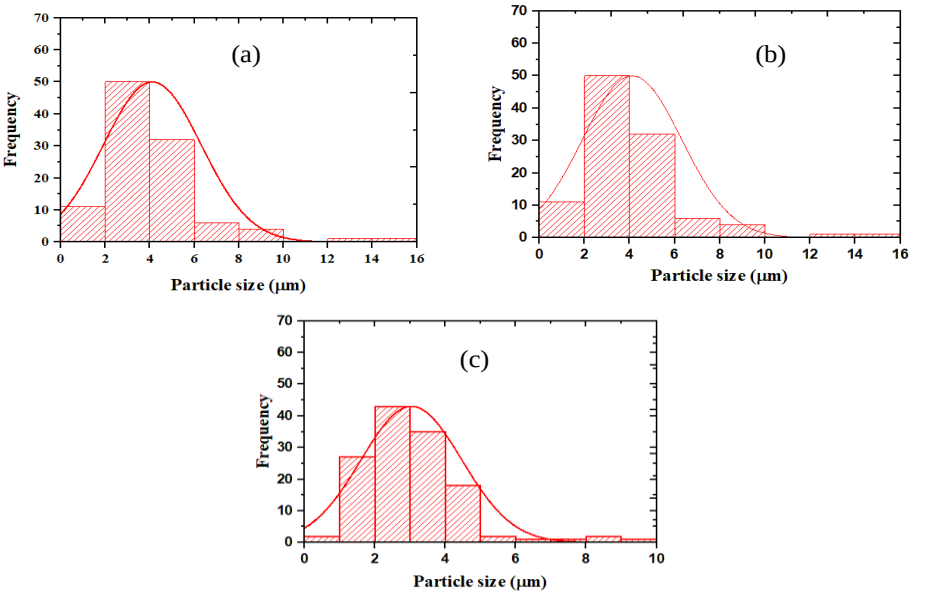

Fig. 14 PM_{10} particle size distribution curves at different sampling periods. (a) normal development date, (b) and (c) date of pyrotechnic events.

and prismatic morphologies respectively, provides clues about their formation processes and origin. This is fundamental for the design of emission control policies. On the other hand, aluminosilicates and silicates, with diverse morphologies and compositions, indicate the influence of both natural sources and human activities, such as construction. Their identification is crucial to understand the long-range transport of particulate matter and its deposition in urban areas, affecting air quality and health.

For the Colombian authorities, the results of the study point to the importance of implementing and strengthening monitoring and control strategies for PM emission sources, given their potential impact on public health. These measures should be complemented with policies that promote the use of clean energy. In addition, it is essential to continue and expand research on both PM_{10} and $PM_{2.5}$ in other cities in the country. For future research, it is recommended to use these analysis techniques (SEM-EDS) as a tool for the detailed study of PM in other urban and rural areas, both in Colombia and in countries facing similar challenges. In countries such as the United States and the European Union, where air quality policies are more stringent, the results can provide a comparative perspective on the effects of various pollution management strategies and control technologies, thus seeking the development and transfer of clean technologies and mitigation strategies.

5. Conclusions

The chemical and morphological characterization of PM_{10} particles carried out in the Aburrá Valley, Colombia, using scanning electron microscopy (SEM) and energy dispersive spectroscopy (EDS) techniques, revealed the diversity and complexity of the atmospheric particles present in tropical urbanized areas. The results obtained allowed the classification of PM_{10} into 11 groups based on their chemical composition and morphological characteristics. The diversity of these groups reflects the variety of emission sources including industrial processes, biomass combustion, vehicular traffic, among others. These results show to the effectiveness of these analytical techniques for understanding the complexity and diversity of PM in urban and industrial environments.

The morphology and chemical composition of PM collected at different sampling stations indicate a significant influence of natural and industrial sources at those stations. This is evidenced by the presence of aluminosilicates, phosphates, carbonates, and biological material, suggesting both anthropogenic and natural source inputs.

Spherical particles such as metal oxides, iron oxides, and fly ash, are of particular concern for air quality and their influence on human health. The fly ash can be recognized by their spherical geometries with smooth surfaces, linked to high-temperature industrial activities adjacent to the MED-MIRA, SUR-TRAF and ITA-POGO stations.

The results of the SEM-EDS analysis highlight the importance of monitoring and characterizing PM due to its potential adverse effects on air quality and public health. The detection of particles with high fractions of harmful elements such as Ni and Fe suggests a potential risk to human health, especially in areas close to heavy industrial sources and heavy

vehicular traffic. It is necessary to develop localized or representative studies of anthropogenic sources, so that chemical and morphological characterization can accurately predict PM emission foci and their diffusion in the AMVA, in order to assess their impact on human health.

It is suggested that additional characterization studies be carried out in the Aburrá Valley using complementary techniques such as X-Ray Diffraction (XRD) and X-Ray Fluorescence (XRF). These techniques will provide a more comprehensive analysis of the microstructure, mineralogy, and chemical composition of the particulate matter (PM). Although Scanning Electron Microscope (SEM) with Energy Dispersive Spectroscopy (EDS) provides elemental and chemical information, this can be complemented and contrasted with XRF, which allows a more detailed chemical analysis of the materials. In addition, the use of XRD will provide information on the microstructure of the PM and allow the composition to be associated with the mineralogical materials present.

Conflict of Interest

There is no conflict of interest.

Supporting Information

Not applicable.

References

[1] J. D. Martínez-Ángel, Motorized mobility, environmental impact, alternatives and future prospects: Considerations for the área metropolitana del valle de aburrá Revista de Salud Publica, 2018, **20**, 126–131, doi: 10.15446/RSAP.V20N1.57038.

[2] A. Baklanov, L. T. Molina, M. Gauss, Megacities, air quality and climate, *Atmospheric Environment*, 2016, **126**, 235-249, doi: 10.1016/j.atmosenv.2015.11.059.

[3] M. A. Correa-Ochoa, J. Rojas, L. M. Gómez, D. Aguiar, C. A. Palacio-Tobón, H. A. Colorado, Systematic search using the proknow-C method for the characterization of atmospheric particulate matter using the materials science techniques XRD, FTIR, XRF, and Raman spectroscopy, *Sustainability*, 2023, **15**, 8504, doi: 10.3390/su15118504.

[4] D. Aguiar-Gil, L. M. Gómez-Peláez, T. Álvarez-Jaramillo, M. A. Correa-Ochoa, J. C. Saldarriaga-Molina, Evaluating the impact of $PM_{2.5}$ atmospheric pollution on population mortality in an urbanized valley in the American tropics, *Atmospheric Environment*, 2020, **224**, 117343, doi: 10.1016/j.atmosenv.2020.117343.

[5] K. K. da Silva, F. T. Duarte, J. N. Rodrigues Matias, S. A. Morais Medeiros Dias, E. de Souza Fernandes Duarte, C. G. Cunha da Silva Soares, J. J. Hoelzemann, M. F. de Oliveira Galvão, Physico-chemical properties and genotoxic effects of air particulate matter collected from a complex of ceramic industries, *Atmospheric Pollution Research*, 2019, **10**, 597-607, doi: 10.1016/j.apr.2018.11.001.

[6] G. Morantes, J. C. González, G. Rincón, Characterisation of particulate matter and identification of emission sources in Greater Caracas, Venezuela, *Air Quality, Atmosphere & Health*, 2021, **14**, 1989-2014, doi: 10.1007/s11869-021-01070-2.

[7] M. A. Correa, S. A. Franco, L. M. Gómez, D. Aguiar, H. A. Colorado, Characterization methods of ions and metals in particulate matter pollutants on $PM_{2.5}$ and PM_{10} samples from several emission sources, *Sustainability*, 2023, **15**, 4402, doi: 10.3390/su15054402.

[8] M. A. Correa-Ochoa, R. Bedoya, L. M. Gómez, D. Aguiar, C. A. Palacio-Tobón, H. A. Colorado, A review on the characterization and measurement of the carbonaceous fraction of particulate matter, *Sustainability*, 2023, **15**, 8717, doi: 10.3390/su15118717.

[9] A. S. Pipal, R. Jan, P. G. Satsangi, S. Tiwari, A. Taneja, Study of surface morphology, elemental composition and origin of atmospheric aerosols ($PM_{2.5}$ and PM_{10}) over Agra, India, *Aerosol and Air Quality Research*, 2014, **14**, 1685-1700, doi: 10.4209/aaqr.2014.01.0017.

[10] S. Yadav, P. G. Satsangi, Chemical and morphological study of PM_{10} and $PM_{2.5}$ in Pune, India, *International Journal of Environment and Waste Management*, 2014, **13**, 199, doi: 10.1504/ijewm.2014.059617.

[11] M. A. Correa-Ochoa, L. C. Vélez-Monsalve, J. C. Saldarriaga-Molina, M. M. Jaramillo-Ciro, Evaluation of the index of atmospheric purity in an american tropical valley through the sampling of corticulous lichens in different phorophyte species, *Ecological indicators*, 2020, **115**, 106355, doi: 10.1016/j.ecolind.2020.106355.

[12] L. M. Gómez Peláez, J. M. Santos, T. T. de Almeida Albuquerque, N. C. Reis Jr, W. L. Andreão, M. de Fátima Andrade, Air quality status and trends over large cities in South America, *Environmental Science & Policy*, 2020, **114**, 422-435, doi: 10.1016/j.envsci.2020.09.009.

[13] S. A. Franco C., M. A. Correa, D. A. G., L. M. Gómez y H. A. Colorado, Characterization and source apportionment of ion and metals in pm10 in an urbanized valley in the american tropics using principal component analysis and positive matrix factorization, *Engineered Science*, 2024, **30**, 1154 doi: 10.30919/es1154.

[14] N. Roldán Henao, Direct and indirect efects of precipitation on particulate matter concentrations in the Aburrá valley, degree thesis, *Universidad Nacional de Colombia*, Medellin, Colombia, 2017.

[15] D. Huckebrink, J. Finke, V. Bertsch, How user behaviour

affects emissions and costs in residential energy systems—The impacts of clothing and thermal comfort, *Environmental Research Communications*, 2023, **5**, 115009, doi: 10.1088/2515-7620/ad0990.

[16] Y. Mancilla, G. Medina, L. T. González y A. Mendoza, Fine particles emission source profiles for a semi-arid urban center: key markers and similarity tests, *Revista Internacional de Contaminación Ambiental*, 2022, **38**, 57–80, doi: 10.20937/rica.54132.

[17] T. R. Oke, G. Mills, A. Christen, J. A. Voogt, Urban Climates. Cambridge, UK: Cambridge University Press, 2017.

[18] F. Karaca, I. Anil, A. Yildiz, Physicochemical and morphological characterization of atmospheric coarse particles by SEM/EDS in new urban central districts of a megacity, *Environmental Science and Pollution Research*, 2019, **26**, 24020-24033, doi: 10.1007/s11356-019-05762-2.

[19] L. T. González, F. E. L. Rodríguez, M. Sánchez-Domínguez, C. Leyva-Porras, L. G. Silva-Vidaurri, K. Acuna-Askar, B. I. Kharisov, J. F. Villarreal Chiu, J. M. Alfaro Barbosa, Chemical and morphological characterization of TSP and $PM_{2.5}$ by SEM-EDS, XPS and XRD collected in the metropolitan area of Monterrey, Mexico, *Atmospheric Environment*, 2016, **143**, 249-260, doi: 10.1016/j.atmosenv.2016.08.053.

[20] J. I. Huertas, M. E. Huertas, D. A. Solís, Characterization of airborne particles in an open pit mining region, *Science of the Total Environment*, 2012, **423**, 39-46, doi: 10.1016/j.scitotenv.2012.01.065.

[21] N. M. Hamdan, H. Alawadhi, X-ray diffraction as a major tool for the analysis of $PM_{2.5}$ and PM_{10} aerosols, *Powder Diffraction*, 2020, **35**, 98-103, doi: 10.1017/s0885715620000184.

[22] H. Ahmady-Birgani, H. Mirnejad, S. Feiznia, K. G. McQueen, Mineralogy and geochemistry of atmospheric particulates in western Iran, *Atmospheric Environment*, 2015, **119**, 262-272, doi: 10.1016/j.atmosenv.2015.08.021.

[23] P. G. Satsangi, S. Yadav, Characterization of $PM_{2.5}$ by X-ray diffraction and scanning electron microscopy–energy dispersive spectrometer: its relation with different pollution sources, *International Journal of Environmental Science and Technology*, 2014, **11**, 217-232, doi: 10.1007/s13762-012-0173-0.

[24] L. T. González, F. E. Longoria-Rodríguez, M. Sánchez-Domínguez, C. Leyva-Porras, K. Acuña-Askar, B. I. Kharissov, A. Arizpe-Zapata, J. M. Alfaro-Barbosa, Seasonal variation and chemical composition of particulate matter: a study by XPS, ICP-AES and sequential microanalysis using Raman with SEM/EDS, *Journal of Environmental Sciences*, 2018, **74**, 32-49, doi: 10.1016/j.jes.2018.02.002.

[25] S. Choung, J. Oh, W. S. Han, C. M. Chon, Y. Kwon, D. Y. Kim, W. Shin, Comparison of physicochemical properties between fine ($PM_{2.5}$) and coarse airborne particles at cold season in Korea, *Science of the Total Environment*, 2016, **541**, 1132-1138, doi: 10.1016/j.scitotenv.2015.10.021.

[26] Y. Huang, L. Wang, S. Zhang, M. Zhang, J. Wang, X. Cheng, T. Li, M. He, S. Ni, Source apportionment and health risk assessment of air pollution particles in eastern district of Chengdu, *Environmental Geochemistry and Health*, 2020, **42**, 2251-2263, doi: 10.1007/s10653-019-00495-0.

[27] D. Roy, G. Singh, N. Gosai, Identification of possible sources of atmospheric PM_{10} using particle size, SEM-EDS and XRD analysis, Jharia Coalfield Dhanbad, India, *Environmental Monitoring and Assessment*, 2015, **187**, 680, doi: 10.1007/s10661-015-4853-3.

[28] A. S. Pipal, P. Gursumeeran Satsangi, Study of carbonaceous species, morphology and sources of fine ($PM_{2.5}$) and coarse (PM_{10}) particles along with their climatic nature in India, *Atmospheric Research*, 2015, **154**, 103-115, doi: 10.1016/j.atmosres.2014.11.007.

[29] C. Yin, X. Cheng, X. Liu, M. Zhao, Identification and classification of atmospheric particles based on SEM images using convolutional neural network with attention mechanism, *Complexity*, 2020, **2020**, 9673724, doi: 10.1155/2020/9673724.

[30] T. Siciliano, R. Giua, M. Siciliano, S. Di Giulio, A. Genga, The morphology and chemical composition of the urban PM_{10} near a steel plant in Apulia determined by scanning electron microscopy. Source Apportionment, *Atmospheric Research*, 2021, **251**, 105416, doi: 10.1016/j.atmosres.2020.105416.

[31] L. C. Palacio, G. Durango-Giraldo, C. Zapata-Hernandez, G. A. Santa-González, D. Uribe, J. Saiz, R. Buitrago-Sierra, C. Tobón, Characterization of airborne particulate matter and its toxic and proarrhythmic effects: a case study in Aburrá Valley, Colombia, *Environmental Pollution*, 2023, **336**, 122475, doi: 10.1016/j.envpol.2023.122475.

[32] D. Marin-Palma, J. D. González, J. F. Narváez, J. Porras, N. A. Taborda, J. C. Hernandez, Physicochemical characterization and evaluation of the cytotoxic effect of particulate matter (PM_{10}), *Water, Air, & Soil Pollution*, 2023, **234**, 138, doi: 10.1007/s11270-023-06155-5.

[33] J. Murillo-Escobar, J. P. Sepulveda-Suescun, M. A. Correa, D. Orrego-Metaute, Forecasting concentrations of air pollutants using support vector regression improved with particle swarm optimization: case study in Aburrá Valley, Colombia, *Urban Climate*, 2019, **29**, 100473, doi: 10.1016/j.uclim.2019.100473.

[34] Departamento Administrativo Nacional de Estadísticas (DANE) - Colombia, Resultados Censo Nacional de Pobla-ción y Vivienda 2018.

[35] C. D. Hoyos, L. Herrera-Mejía, N. Roldán-Henao y A. Isaza, Effects of fireworks on particulate matter concentration in a narrow valley: the case of the Medellín metropolitan area, *Environmental Monitoring and Assessment*, 2019, **192**, 6, doi

10.1007/s10661-019-7838-9.

[36] K. Martinello, M. L. S. Oliveira, F. A. Molossi, C. G. Ramos, E. C. Teixeira, R. M. Kautzmann, L. F. O. Silva, Direct identification of hazardous elements in ultra-fine and nanominerals from coal fly ash produced during diesel co-firing, *Science of the Total Environment*, 2014, **470**, 444-452, doi: 10.1016/j.scitotenv.2013.10.007.

[37] N. M. Hamdan, H. Alawadhi, M. Shameer, Characterization of $PM_{2.5}$ at a traffic site using several integrated analytical techniques, *X-Ray Spectrometry*, 2021, **50**, 106-120, doi: 10.1002/xrs.3201.

[38] S. Canepari, C. Perrino, F. Olivieri, M. L. Astolfi, Characterisation of the traffic sources of PM through size-segregated sampling, sequential leaching and ICP analysis, *Atmospheric Environment*, 2008, **42**, 8161-8175, doi: 10.1016/j.atmosenv.2008.07.052.

[39] T. Siciliano, R. Giua, M. Siciliano, S. Di Giulio, A. Genga, The morphology and chemical composition of the urban PM_{10} near a steel plant in Apulia determined by scanning electron microscopy. Source Apportionment, *Atmospheric Research*, 2021, **251**, 105416, doi: 10.1016/j.atmosres.2020.105416.

[40] L. Herrera-Mejía y C. D. Hoyos, Characterization of the atmospheric boundary layer in a narrow tropical valley using remote-sensing and radiosonde observations and the WRF model: the aburrá valley case-study, *Quarterly Journal of the Royal Meteorological Society*, 2019, **145**, 2641–2665, doi: 10.1002/qj.3583.

[41] S. Ganiger, S. S. Patil, H. P. Dasari, R. Priyanka, S. Kollimarla, Printex-U soot oxidation kinetic behaviour over Alumina and Quartz, *Chemical Engineering Science*, 2022, **247**, 117016, doi: 10.1016/j.ces.2021.117016.

[42] N. M. Hamdan, H. Alawadhi, X-ray diffraction as a major tool for the analysis of $PM_{2.5}$ and PM_{10} aerosols, *Powder Diffraction*, 2020, **35**, 98-103, doi: 10.1017/s0885715620000184.

[43] S. Yadav, P. G. Satsangi, Chemical and morphological study of PM_{10} and $PM_{2.5}$ in Pune, India, *International Journal of Environment and Waste Management*, 2014, **13**, 199, doi: 10.1504/ijewm.2014.059617.

[44] M. Santacatalina, C. Reche, M. C. Minguillón, A. Escrig, V. Sanfelix, A. Carratalá, J. F. Nicolás, E. Yubero, J. Crespo, A. Alastuey, Impact of fugitive emissions in ambient PM levels and compositionA case study in Southeast Spain, *Science of the Total Environment*, 2010, **408**, 4999-5009, doi: 10.1016/j.scitotenv.2010.07.040.

[45] J. Saikia, B. Narzary, S. Roy, M. Bordoloi, P. Saikia, B. K. Saikia, Nanominerals, fullerene aggregates, and hazardous elements in coal and coal combustion-generated aerosols: an environmental and toxicological assessment, *Chemosphere*, 2016, **164**, 84-91, doi: 10.1016/j.chemosphere.2016.08.086.

[46] X. Querol, A. Alastuey, J. Puicercus, E. Mantilla, C. R. Ruiz, A. Lopez-Soler, F. Plana, R. Juan, Seasonal evolution of suspended particles around a large coal-fired power station: chemical characterization, *Atmospheric Environment*, 1998, **32**, 719-731, doi: 10.1016/s1352-2310(97)00340-3.

[47] H. T. Cujia, Evaluación de la variación vertical del contenido de azufre en mantos de carbón del municipio de Puerto Libertador, Córdoba, degree thesis, Univ. Nac. Colomb., Medellin, Colombia 2019.

[48] A. A. Hashem, S. A. Mahmoud, R. A. Geioushy, O. A, Fouad, Adsorption of malachite green dye over synthesized calcium silicate nanopowders from waste materials, *Materials Science and Engineering: B*, 2023, **295**, 116605, doi: 10.1016/j.mseb.2023.116605

[49] N. Roldán-Henao, C. D. Hoyos, L. Herrera-Mejía y A. Isaza, An investigation of the precipitation net effect on the particulate matter concentration in a narrow valley: role of lower-troposphere stability, *Journal of Applied Meteorology and Climatology*, 2020, **59**, 401–426, doi: 10.1175/jamc-d-18-0313.1

[50] H. Xu, W. Song, W. Cao, G. Shao, H. Lu, D. Yang, D. Chen, R. Zhang, Utilization of coal gangue for the production of brick, *Journal of Material Cycles and Waste Management*, 2017, **19**, 1270-1278, doi: 10.1007/s10163-016-0521-0.

[51] T. B. H. Schroeder, J. Houghtaling, B. D. Wilts, M. Mayer, It's not a bug, it's a feature: functional materials in insects, *Advanced Materials*, 2018, **30**, 1705322, doi: 10.1002/adma.201705322.

[52] T. Moreno, Atmospheric aerosols: environmental issues. *Environmental issues*, 2007.

[53] B. Jin, X. Wu, D. Weng, S. Liu, T. Yu, Z. Zhao, Y. Wei, Roles of cobalt and cerium species in three-dimensionally ordered macroporous Co Ce1-O catalysts for the catalytic oxidation of diesel soot, *Journal of Colloid and Interface Science*, 2018, **532**, 579-587, doi: 10.1016/j.jcis.2018.08.018.

[54] M. Zhao, J. Deng, J. Liu, Y. Li, J. Liu, Z. Duan, J. Xiong, Z. Zhao, Y. Wei, W. Song, Y. Sun, Roles of surface-active oxygen species on 3DOM cobalt-based spinel catalysts $M_xCo_{3-x}O_4$ (M = Zn and Ni) for NO_x-assisted soot oxidation, *ACS Catalysis*, 2019, **9**, 7548-7567, doi: 10.1021/acscatal.9b01995.